Chemical Modification of Paclitaxel (Taxol) Reduces P-Glycoprotein Interactions and Increases Permeation across the Blood−Brain Barrier in Vitro and in Situ

Antonie Rice,[†] Yanbin Liu,[‡] Mary Lou Michaelis,[§] Richard H. Himes,[||] Gunda I. Georg,[‡] and Kenneth L. Audus*[,†]

Department of Pharmaceutical Chemistry, University of Kansas, 226 Simons, 2095 Constant Avenue, Lawrence, Kansas 66047, Department of Pharmacology and Toxicology, University of Kansas, Malott Hall 5064, 1251 Wescoe Hall Drive, Lawrence, Kansas 66045, Department of Medicinal Chemistry, University of Kansas, Malott Hall 4070, 1251 Wescoe Hall Drive, Lawrence, Kansas 66045, and Department of Molecular Biosciences, University of Kansas, Haworth Hall 2034, 1200 Sunnyside Avenue, Lawrence, Kansas 66045

Received June 10, 2004

The purpose of this work was to introduce a chemical modification into the paclitaxel (Taxol) structure to reduce interactions with the product of the multidrug resistant type 1 (MDR1) gene, P-glycoprotein (Pgp), resulting in improved blood−brain barrier (BBB) permeability. Specifically, a taxane analogue, Tx-67, with a succinate group added at the C10 position of Taxol, was synthesized and identified as such a candidate. In comparison studies, Tx-67 had no apparent interactions with Pgp, as demonstrated by the lack of enhanced uptake of rhodamine 123 by brain microvessel endothelial cells (BMECs) in the presence of the agent. By contrast, Taxol exposure substantially enhanced rhodamine 123 uptake by BMECs through inhibition of Pgp. The transport across BMEC monolayers was polarized for both Tx-67 and Taxol with permeation in the apical to basolateral direction greater for Tx-67 and substantially reduced for Taxol relative to basolateral to apical permeation. Taxol and cyclosporin A treatments also did not enhance Tx-67 permeation across BMEC monolayers. In an in situ rat brain perfusion study, Tx-67 was demonstrated to permeate across the BBB at a greater rate than Taxol. These results demonstrate that the Taxol analogue Tx-67 had a reduced interaction with Pgp and, as a consequence, enhanced permeation across the blood−brain barrier in vitro and in situ.

Introduction

Paclitaxel (Taxol) is one of the most active cancer chemotherapeutic agents known.[1−5] At present, it is commonly used for the treatment of breast and ovarian cancers. Taxol causes cells to arrest at the G_2/M phase of the cell cycle through drug-induced tubulin polymerization and microtubule stabilization, thus leading to induced cell apoptosis.[6−9]

Previous studies have established that Taxol is not significantly absorbed across the gastrointestinal epthelium after oral administration[10,11] and does not cross the blood−brain barrier (BBB).[12−14] A primary mechanism limiting Taxol distribution into the brain is active efflux by the multidrug resistant gene product 1 (MDR1) or P-glycoprotein (Pgp) localized on the blood side of the microcerebrovascular endothelium comprising the BBB. Permeation of Taxol across these tissues may be substantially improved by inhibiting Pgp-mediated efflux.[13,14]

Ojima et al.[15] have observed that there is a specific binding site for taxoids on Pgp. Accordingly, by modifying specific moieties on the Taxol molecule, new taxanes might be identified with reduced binding or recognition by Pgp and potentially enhanced permeability properties with respect to crossing the BBB. The hypothesis by Seelig[1] also holds that there are differences in affinity for Pgp among structurally similar molecules. These differences are characterized by fixed spatial separations of pairs of recognition elements, type I and type II, that have different strengths to be electron donors or acceptor groups. It is believed that these differences could be exploited by chemical modification of the recognition elements. That is, by chemical modification, the recognition elements on a particular molecule would be decreased and the entity's strength for Pgp binding thus reduced. Seelig further observed that type I units with negative charge, such as the carboxylic acids group (e.g., *S*-farnesylcysteine and reserpic acid), the sulfonyl group (e.g., trypan blue), or the mesomeric nitro group (e.g., flunitrazepam), do not interact with Pgp. On the other hand, chemical structures that bear type I units in addition to the negatively charged groups are substrates (e.g., cefoperazone or morphine-6-glucoronide).[1]

The objective of these studies was to characterize the transport of Taxol and a novel taxane, Tx-67, with potentially reduced Pgp interactions, both in vitro and in situ. The structures of Taxol and Tx-67 are shown in Figure 1. In this new taxane, the introduction of the succinate removed apparent Pgp interactions, despite the fact that the molecule has other type I and type II units. This could be due to the fact that the interactions at the C10 position are particularly important for Pgp interaction.

* Corresponding author. Phone: 785-864-3591. Fax: 785-864-5265. E-mail: audus@ku.edu.
[†] Department of Pharmaceutical Chemistry.
[‡] Department of Medicinal Chemistry.
[§] Department of Pharmacology and Toxicology.
[||] Department of Molecular Biosciences.

10.1021/jm040114b CCC: $30.25
Published on Web 01/05/2005

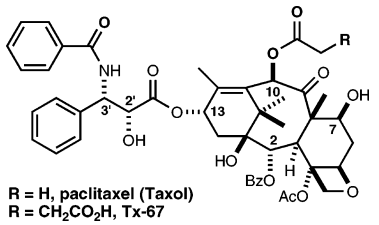

Figure 1. Chemical structures for Taxol and Tx-67.

Scheme 1

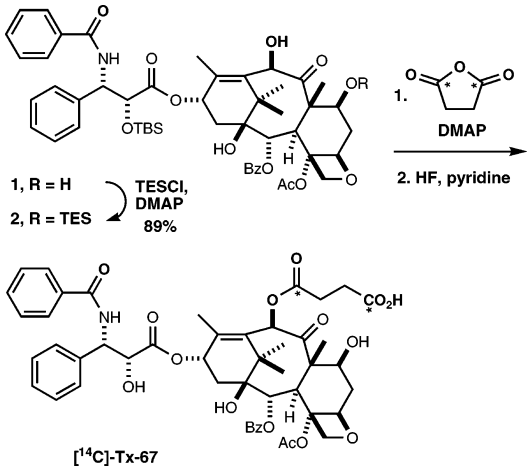

Materials and Methods

[^{14}C]Sucrose (specific activity 401 mCi/mmol), [^{3}H]Taxol (specific activity 10.5 Ci/mmol), [^{3}H]sucrose (specific activity 40 mCi/mmol), cell culture medium, 100-mm culture dishes, 0.4-μm-pore polycarbonate filters (13 mm diameter), cyclosporin A (CsA), penicillin G, amphotericin B, endothelial cell growth supplement, and fibronectin were all commercially available.

Synthesis of [^{14}C]TX-67. The radioactive C10 monosuccinate [^{14}C]TX-67 was prepared in two steps (Scheme 1) from 2′-*O*-(*tert*-butyldimethylsilyl)-10-deacetylpaclitaxel (**1**).[16] Selective silylation of **1** at O7 with triethylsilyl chloride provided 2′,7-bis-silylated intermediate **2**, which was reacted with 1,4-^{14}C-succinic anhydride, followed by desilylation to yield [^{14}C]-TX-67. In this reaction, a large excess of the taxane relative to the ^{14}C-labeled succinic anhydride was used because of the high cost of the radioactive reagent. [^{14}C]TX-67 (2.9 mg) was prepared with a specific activity of 42 mCi/mmol.

2′-*O*-(*tert*-Butyldimethylsilyl)-10-*O*-deacetyl-7-*O*-triethylsilylpaclitaxel (1). To a solution of 2′-*O*-(*tert*-butyldimethylsilyl)-10-*O*-deacetylpaclitaxel[16] (0.025 g, 0.027 mmol) in CH_2Cl_2 (1.0 mL) were added DMAP (0.033 g, 0.27 mmol) and chlorotriethylsilane (0.045 mL, 0.27 mmol). The mixture was stirred at room temperature for 5 h and then diluted with CH_2Cl_2 (10 mL). This mixture was washed with a saturated NH_4Cl solution (5.0 mL) and water (5.0 mL). The organic layer was dried over Na_2SO_4. Removal of solvent followed by flash chromatography on silica gel (EtOAc−hexane, 1:3) provided the title compound as a colorless solid (0.024 g, 89% yield): ^{1}H NMR (300 MHz, $CDCl_3$) δ −0.26 (s, 3H, $SiCH_3$), −0.02 (s, 3H, $SiCH_3$), 0.50−0.62 (m, 6H, $Si(CH_2CH_3)_3$), 0.80 (s, 9H, *tert*-butyl), 0.94 (t, J = 7.8 Hz, 9H, $Si(CH_2CH_3)_3$), 1.10 (s, 3H, H17), 1.22 (s, 3H, H16), 1.76 (s, 3H, H19), 1.93 (s, 3H, H18), 1.92−2.14 (m, 2H, H6), 2.3 and 2.56 (m, 2H, H14), 2.58 (s, 3H, 4-Ac), 3.91 (d, J = 6.9 Hz, 1H, H3), 4.23 (d, J = 8.1 Hz, 1H, H20), 4.30 (d, J = 1.8 Hz, 1H, 10-OH), 4.35 (d, J = 8.1 Hz, 1H, H20), 4.42 (dd, J = 6.6 and 10.8 Hz, 1H, H7), 4.68 (d, J = 2.1 Hz, 1H, H2′), 4.98 (dd, J = 1.5 and 9.3 Hz, 1H, H5), 5.13 (d, J = 1.8 Hz, 1H, H10), 5.69 (d, J = 6.9 Hz, 1H, H2), 5.73 (dd, J = 1.8 and 9 Hz, 1H, H3′), 6.34 (t, J = 8.7 Hz, 1H, H13), 7.11 (d, J = 9 Hz, 1H, NH), 7.33−8.16 (m, 15H); ^{13}C NMR (75 MHz, $CDCl_3$) δ 5.6, 7.2, 10.5, 14.7, 18.5, 21.4, 23.5, 25.9, 27.0, 36.3, 37.6, 43.6, 46.8, 56.6, 58.1, 71.8, 73.2, 74.4, 75.4, 75.5, 79.3, 81.5, 84.6, 126.8, 127.4, 129.1, 129.2, 130.6, 132.1, 134.0, 134.4, 136.5, 138.5, 138.7, 167.3, 167.4, 170.6, 171.7, 210.2; HRMS (FAB) *m/z* calcd for $C_{57}H_{78}NO_{13}Si_2$ (M + 1) 1040.5012, found 1040.5019.

[^{14}C]-10-*O*-Succinyl Mono Ester of 10-*O*-Deacetylpaclitaxel ([^{14}C]TX-67). Step 1. Using dry toluene (3 × 0.5 mL), commercially available 1,4-^{14}C-succinic anhydride (specific activity 50 mCi/mmol, approximately 1.0−0.4 mg, 0.010−0.004 mmol) was transferred into a 10 mL round-bottom reaction flask containing a stirring bar. To this solution were added 2′-*O*-(*tert*-butyldimethylsilyl)-10-*O*-deacetyl-7-*O*-triethylsilylpaclitaxel (**2**, 62 mg, 0.0596 mmol) and DMAP (4.9 mg, 0.04 mmol). The reaction vial was capped and the reaction was heated at 85−90 °C for 20 h until the completion of the reaction (monitored by TLC). After cooling to room temperature, the reaction mixture was placed into a top-screwed test tube containing CH_2Cl_2 (5 mL) and aqueous HCl (0.2%, 5 mL). The reaction vessel was washed with additional CH_2Cl_2 (2 mL), which was also collected in the test tube. The aqueous layer was removed and extracted twice with CH_2Cl_2 (2 mL each). The aqueous layer was discarded. The organic layer was dried over sodium sulfate. The solvent was then removed and the residue was purified by column chromatography using silica gel (3% methanol in chloroform) to yield 3.9 mg of the acylated reaction product.

Step 2. The acylated reaction product was transferred into a Teflon vial using CH_2Cl_2 (5 × 1 mL). The solvent was removed slowly from the vial by a flow of argon. The residue was dissolved in pyridine (1.0 mL) and cooled to 0 °C. After the addition of six drops of HF/pyridine, the ice bath was removed and the mixture was stirred at 25 °C for 5 h. The reaction mixture was then placed into a top-screwed test tube containing CH_2Cl_2 (5 mL) and 2% aqueous HCl (5 mL). The aqueous layer was discarded. The organic layer was washed twice with aqueous HCl (2%, 2 × 5 mL) and then dried over magnesium sulfate. Removal of the solvent under reduced pressure, followed by drying on a vacuum pump overnight, yielded 2.9 mg (specific activity 42 mCi/mmol) of the target compound [^{14}C]Tx-67.

Tx-67 was first prepared using the conditions described above with nonradioactive succinic anhydride. All spectroscopic data for Tx-67, prepared under those conditions, were identical to those previously reported for Tx-67.[17] The radioactive product [^{14}C]Tx-67 was compared to TX-67 using thin-layer chromatography and several different solvent systems.

Analytical data for Tx-67, 10-*O*-Deacetylpaclitaxel 10-monosuccinyl ester: ^{1}H NMR (300 MHz, $CDCl_3$) δ 1.12 (s, 3H), 1.25 (s, 3H), 1.64 (s, 3H), 1.78 (s, 3H), 1.81−1.87 (m, 1H), 2.20−2.72 (m, 7H), 2.35 (s, 3H), 3.76 (d, J = 6.9 Hz, 1H), 4.20 and 4.27 (d, J = 8.4 Hz, 2H), 4.36 (dd, J = 6.9 and 10.5 Hz, 1H), 4.78 (d, J = 3 Hz, 1H), 4.92 (d, J = 8.7 Hz, 1H), 5.65 (d, J = 6.9 Hz, 1H), 5.75 (dd, J = 2.4 and 8.7 Hz, 1H), 6.19 (t, J = 9.0 Hz, 1H), 6.25 (s, 1H), 7.18 (d, J = 9.0 Hz, 1H), 7.27−8.11 (m, 15H); ^{13}C NMR (75 MHz, $CDCl_3$) δ 9.6, 14.7, 21.0, 22.6, 28.9, 29.0, 35.6, 43.0, 45.7, 55.1, 58.4, 72.0, 72.1, 73.1, 75.0, 75.8, 78.9, 81.1, 84.4, 127.0, 127.1, 128.2, 128.6, 128.7, 128.9, 129.2, 130.2, 131.9, 133.0, 133.6, 138.0, 142.2, 166.8, 167.5, 168.0, 170.3, 172.3, 172.6, 203.5; HRMS *m/z* calcd for $C_{49}H_{54}NO_{16}$ (M + 1) 912.3364, found 912.3350. The purity was verified as 96−99% by HPLC. HPLC conditions were as follows: Vydac C18 column (5 μm, 10 × 250 mm), UV detection at 280 nM, and gradient elution with 0.1% aqueous trifluoroacetic acid and 0−100% acetonitrile in 0.1% trifluoroacetic acid for 40 min. Retention time was 24.8 min.

Cell Culture. Bovine brain microvessel endothelial cells (BMECs) were isolated and grown in primary culture and characterized as detailed by Audus et al.[18,19]

Rhodamine 123 Uptake Assay. BMECs were seeded onto 12-well cluster dishes at a density of 50 000 cells/cm^2. The culture medium was changed every other day after seeding until a confluent monolayer was formed as determined by light microscopy. Experiments were performed in phosphate-buffered saline supplemented with calcium and glucose (PBSA),

pH 7.4, essentially as detailed earlier by Rose et al.[20] Briefly, the growth medium was first aspirated off and then the cells were rinsed three times with prewarmed (37 °C) PBSA. The monolayers were then either equilibrated in 1 mL of PBSA for 1 h at 37 °C for control experiments or equilibrated for 30 min in PBSA alone, followed by another 45 min preincubation with the a taxane. Cyclosporin A (CsA; 10 μM) was used as a known Pgp inhibitor and as the positive control. Rhodamine 123 accumulation was then performed for 45 min with or without a potential inhibitor present with gentle agitation (~30 rpm) at 37 °C. At the end of the experiment, the drug solution was removed by aspiration, and the monolayers were immediately rinsed three times with ice-cold PBSA. Each monolayer was solubilized for 30 min (37 °C) with 1 mL of lysing solution (0.5% v/v Triton X-100 in 0.2 N NaOH). Cell lysates were assayed using a microplate fluorescence reader (Bio-Tek Instruments, Winooski, VT) at excitation/emission wavelengths of 485 nm/520 nm and then quantified against standard curves of rhodamine 123 in lysing solution. The fluorescence of the cell lysates was corrected for autofluorescence of untreated cells. The protein content of each monolayer was then determined using the BCA protein assay reagent kit. Results were expressed as total moles of rhodamine 123 accumulation per microgram of cellular protein.

Permeation of Taxanes across BBMEC Monolayers. BMECs were grown on 0.4 μm polycarbonate membranes. Upon confluency, the cells were transferred to side-by-side diffusion chambers as detailed by Audus et al.[18,19] to characterize the transport of [^{3}H]Taxol or [^{14}C]Tx-67. Transport studies were performed in pH 7.4 standard buffer solutions, consisting of either Hank's balanced salt solution (HBSS) or phosphate-buffered saline (PBS) supplemented with 0.63 mM $CaCl_2$, 0.74 mM $MgSO_4$, 5.3 mM glucose, and 0.1 mM ascorbic acid (PBSA). Briefly, all studies were performed in 3 mL of PBSA in each donor and receiver chamber of the side-by-side diffusion chambers and stirred at 600 rpm at 37 °C. The cells were allowed to equilibrate in PBSA for 30 min prior to each experiment and oriented such that the apical or blood side of the cells face the donor chamber and the basolateral or brain side of the cells adhere to the polycarbonate membranes and face the receiver chamber of the diffusion apparatus. At each time point, a 100 μL sample was taken from the receiver compartment and immediately replaced with an equal volume of PBSA. The transport studies were performed in the presence or absence of CsA (5−10 μM). Monolayers were checked for trypan blue exclusion after experiments as well to assess general cell viability. The permeability of all monolayers used in these experiments was monitored for [^{14}C] sucrose leakage as a measure of potential taxane-induced loss of integrity. The radioactivity was quantified using liquid scintillation spectrometry. Apparent permeability coefficients (P_{app}) were calculated as detailed by Adson et al.[21]

Determination of Concentration Dependence for Taxol and Tx-67 Efflux by Pgp Efflux Pump. Cells were grown and transport studies were set up as described in the previous section. Permeation studies were performed in the presence of ranges of concentrations of [^{3}H]Taxol (1 nM to 25 μM) and [^{14}C]Tx-67 (1−250 nM). Sucrose transport was determined for each permeation study. Transport studies were performed for 2 h. The radioactivity was quantified using liquid scintillation spectrometry. Apparent permeability coefficients (P_{app}) were calculated.

In other experiments, permeation studies were performed to determine if Tx-67 transport was inhibited by P-glycoprotein inhibitors. The bidirectional flux was evaluated for [^{14}C]Tx-67 in the presence of unlabeled Taxol (25 μM) and CSA (5−10 μM).

In Situ Rat Brain Perfusion of Taxol and Tx-67. Adult male Sprague−Dawley rats, weighing 250−350 g, were obtained from Sasco. The in situ rat brain perfusion technique originally described by Smith and Allen[22] was employed to determine the BBB permeability of Taxol and Tx-67. Animal subjects were maintained and used in these studies with full approval of the University of Kansas Institutional Animal Care and Use Committee. Adult male Sprague−Dawley rats (350−400 g) were anesthetized with a mixture containing 1.5 mL/kg of solution consisting of 37.5 mg/mL ketamine, 1.9 mg/mL xylazine, and 0.37 mg/mL acepromazine. A full dosage was given for the initial anesthesia and one-third of the full dose given for repeated dose at 1-h intervals. After the rat was anesthetized, it was placed on a warm-pad and the temperature was monitored by inserting a thermometer into the rectum, and body temperature was maintained at 37 °C. Briefly, either the right or left common carotid artery was surgically exposed and cannulated for delivery of perfusion fluid (0.9% saline) to the brain. The external carotid was ligated to reduce the amount of perfusion fluid distribution to extracerebral tissues.[22] An individual rat was then perfused with the buffer containing a tracer (sucrose) and the sample (Taxol or Tx-67) for specific time intervals (i.e., for 30, or 60, or 120 s). After the perfusion, the rat was decapitated and the brain was removed for sampling of regions. The brain samples were digested in Solvable for 24 h, and the radioactivity was quantified via liquid scintillation spectrometry. The capillary permeability−surface area product (PA) (mL/s/g) was calculated for both Taxol and Tx-67 by the following equation:

$$PA = -F \ln [1 - C_{br}(T)/FTC_{pf}]$$

where F is the regional cerebral blood flow (mL/s/g), C_{br} represents the concentration of tracer in the brain parenchyma (dpm/g), C_{pf} is the concentration in the perfusion fluid (dpm/mL), and T is the total perfusion time.[22]

Results

Effects of Taxol and Tx-67 on Rhodamine 123 Uptake. The potential interactions of Taxol and Tx-67 with P-glycoprotein, relative to a positive control, CsA, were investigated by assessing rhodamine 123 uptake by BMECs in the presence and absence of the agents. As shown in Figure 2A, Taxol exposure enhanced the BMEC uptake of the P-glycoprotein substrate rhodamine 123. Similarly, in Figure 2B, the positive control CsA enhanced rhodamine 123 uptake by BMECs. In contrast, Tx-67 had no effect on rhodamine 123 uptake by BMECs, suggesting an absence of interactions with P-glycoprotein.

Bidirectional Permeation of Taxol and Tx-67 across BMEC Monolayers. To more directly examine the interactions of Taxol and Tx-67 with the P-glycoprotein directly, the concentration-dependent permeation of Taxol and Tx-67 across BMEC monolayers was investigated for asymmetric, bidirectional permeation that is typical for P-glycoprotein substrates. The apical to basolateral permeation of 1 nM Tx-67 across BMEC monolayers was approximately $9.7 \pm 0.4 \times 10^{-5}$ cm/s and was higher than the inert background permeation marker sucrose at $5.3 \pm 0.8 \times 10^{-5}$ cm/s. The apical to basolateral permeation of 1 nM Taxol across BMEC monolayers was approximately $0.88 \pm 0.9 \times 10^{-5}$ cm/s and was significantly lower than the inert background permeation marker sucrose. Figure 3A shows the permeation curves with increasing concentrations of Taxol in the side-by-side diffusion chamber. At lower concentrations of Taxol (~50−100 nM), the permeability rates were greater for the basolateral to apical direction. At higher concentrations of Taxol, the asymmetry of permeation across the monolayers was lost. Over the concentration range examined, increasing the concentration of Taxol appeared to saturate the transport mechanism and eventually resulted in increased efficiency of permeation (i.e., increased permeability coefficients).

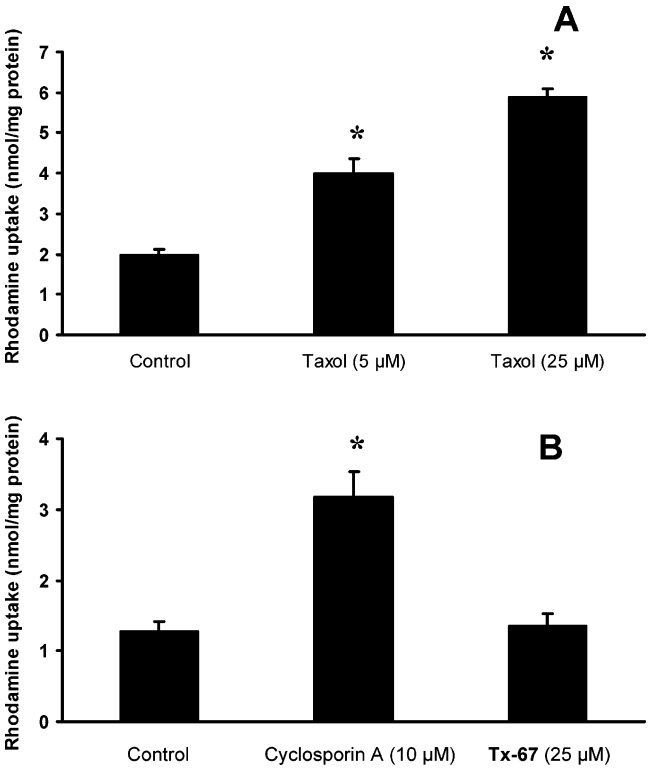

Figure 2. Rhodamine 123 uptake alone and in the presence of (A) Taxol and (B) cyclosporin A and Tx-67 (B). Bars represent the mean ± standard deviation for $n = 3$ different monolayers. *Significant difference, $p < 0.05$, compared to rhodamine uptake in the absence of any treatment (control) as determined by ANOVA.

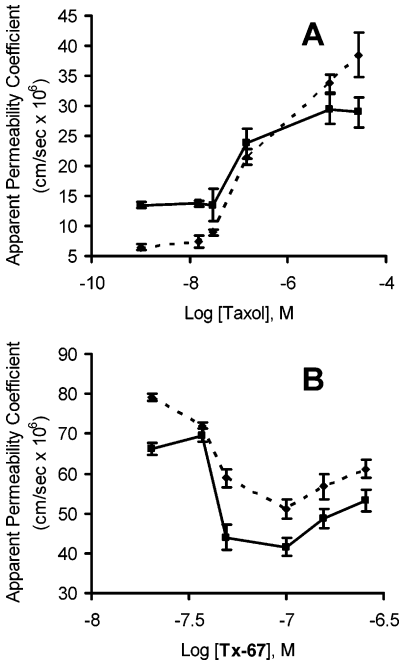

Figure 3. Concentration-dependence of apparent permeability coefficients for the bidirectional permeation of (A) [^{3}H]-Taxol and (B) [^{14}C]Tx-67 across brain microvessel endothelial cell monolayers: - ◆ -, apical to basolateral; −■−, basolateral to apical. Data points represent the mean ± standard deviation for $n = 3$ different monolayers.

Figure 3B shows that in the lower concentration range of Tx-67 (<50 nM) permeation was greater in the apical to basolateral direction. Moreover, Tx-67 permeation across the monolayers was greater than that of Taxol over the entire concentration range examined for the agent. Increasing concentrations of Tx-67 appeared to result in a decreased permeation efficiency (i.e., decreased permeability coefficients) and suggested interactions with a rate-limiting mechanism, possibly another transporter.

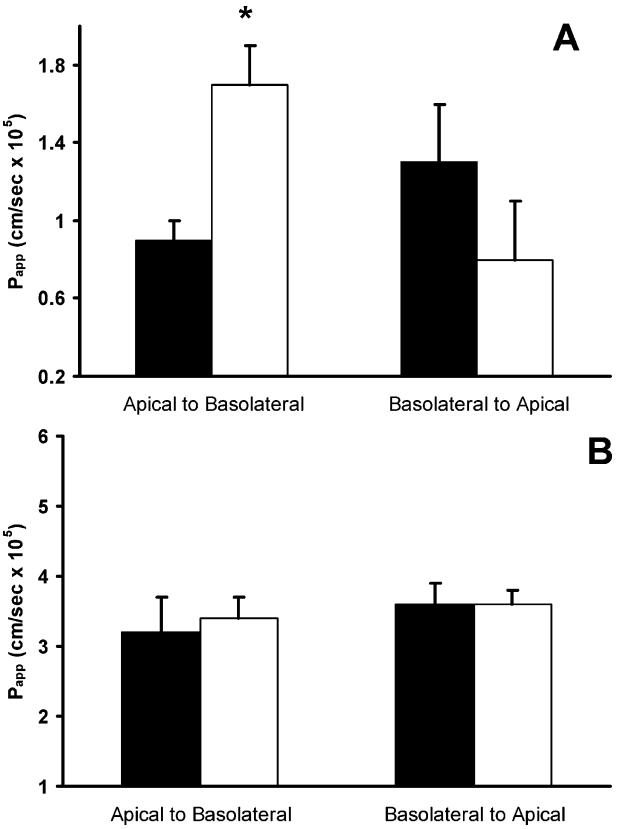

Figure 4. Effect of 10 μM cyclosporine A (CsA) (open bars) on the apparent permeability coefficients (P_{app}) for (A) 10 nM [^{3}H]Taxol (solid bars) and (B) 1 μM [^{3}H]Taxol (solid bars) permeation across brain microvessel endothelial cell monolayers. Data points represent the mean ± standard deviation for $n = 3$ different monolayers. *Significant difference, $p < 0.05$, compared to Taxol alone as determined by ANOVA.

Sucrose permeability was not affected by the increasing concentration of Taxol or Tx-67 at the concentrations used in Figure 3 (data not shown). Additionally, monolayers showed trypan blue exclusion at the conclusion of the transport studies, further confirming that the cells remain viable under the experimental conditions (data not shown).

Pgp has been localized to the apical or blood side of brain microvessel endothelium.[23] To verify in our system that an apically located mechanism consistent with Pgp was involved, we treated the cell monolayers with the Pgp inhibitor CsA. Treatment of BMEC monolayers with the Pgp inhibitor CsA (10 μM) increased the permeation of 10 nM Taxol in the apical to basolateral direction when added to the donor chamber, as shown in Figure 4A, or both donor and receiver chambers (data not shown) during the transport experiments. No significant increase in Taxol permeation was observed in the apical to basolateral direction when CsA was added only to the receiver chamber (data not shown). Taxol permeation was not significantly altered in the basolateral to apical direction when CsA was added either

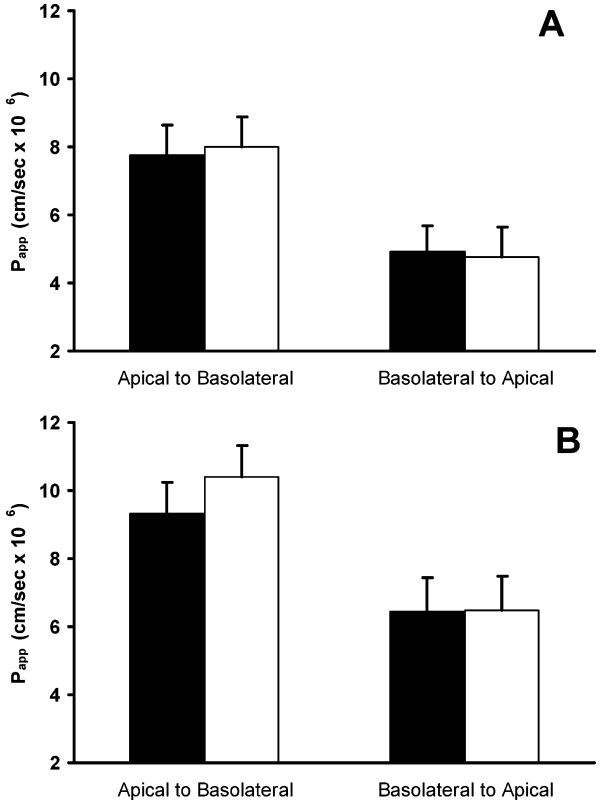

Figure 5. Effect of (A) 10 μM cyclosporine A (CsA; open bars) and (B) 25 μM Taxol (open bars) on the apparent permeability coefficient (P_{app}) for the permeation of 25 nM [^{14}C]Tx-67 (solid bars) across brain microvessel endothelial cell monolayers. Data points represent the mean ± standard deviation for n = 3 different monolayers. *Significant difference, $p < 0.05$, compared to Taxol alone as determined by ANOVA.

to the donor compartment, as illustrated in Figure 4A, or to both compartments (data not shown). These effects were consistent with an apical localization of Pgp and influence on Taxol transport.

Figure 4B shows that treatment of BMEC monolayers with the Pgp inhibitor CsA (10 μM) in the donor chamber of the diffusion apparatus had no effect on the permeation of 1 μM Taxol across BMEC monolayers in either the apical to basolateral direction or the basolateral to apical direction. Addition of CsA to either donor and receiver or receiver alone also was not effective in altering the permeation of the higher concentration of Taxol across BMEC monolayers. These results were consistent with high concentrations of Taxol saturating Pgp and an absence of effects of CsA on permeation.

We investigated the permeation properties of Tx-67 in the presence of CsA and Taxol to further examine the interaction of Tx-67 with Pgp. Figure 5A shows the absence of effects of CsA in the donor chamber of the diffusion apparatus on the permeation of 25 nM Tx-67 across BMEC monolayers in both apical to basolateral and basolateral to apical directions. Similarly, Figure 5B shows the absence of effects of Taxol in the donor chamber of the diffusion apparatus on the permeation of 25 nM Tx-67 across BMEC monolayers in both apical to basolateral and basolateral to apical directions. These results were consistent with a lack of influence of Pgp on Tx-67 permeation across BMEC monolayers.

Table 1. Apparent Permeability Coefficients for [^{14}C]Tx-67 and [^{3}H]Taxol in the in Situ Rat Brain Perfusion Technique[a]

	$P_{app} \times 10^7$ cm/s		
compound	30 s	60 s	120 s
[^{14}C]Tx-67	8.47	13.71	10.75
[^{3}H]Taxol	0.845	1.700	1.574

[a] Time points were for 30, 60, and 120 s (each time point was done in duplicate, n = 2).

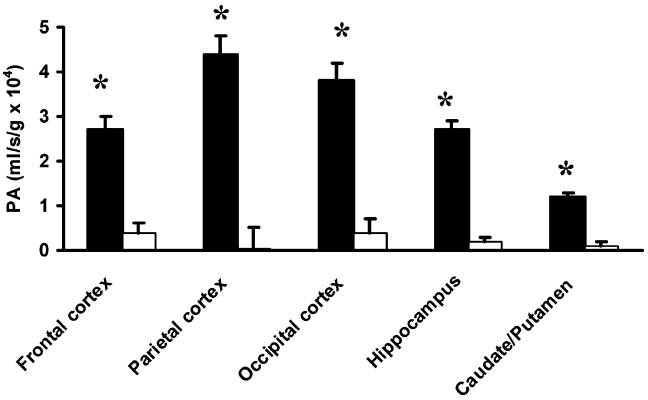

Figure 6. Cerebrovascular permeability−surface area product (PA) for [^{3}H]Taxol (open bars) and [^{14}C]Tx-67 (solid bars), as measured by the brain perfusion technique (60 s data). Data points represent the mean ± standard deviation for n = 3 different rats. *Significant difference, $p < 0.05$, compared to Taxol as determined by ANOVA.

In Situ Rat Brain Perfusion Studies with Tx-67 and Taxol. To verify the in vitro observations regarding enhanced BBB permeation of Tx-67, in situ perfusion experiments were performed with [^{14}C]Tx-67 (300 nM or 0.03 mg/kg) and [^{3}H]Taxol (100 nM or 0.01 mg/kg) at the lowest concentrations allowed by the specific activity of the agents. As summarized in Table 1, we observed a greater P_{app} for Tx-67 than Taxol at each perfusion time. Figure 6 also shows in a separate series of studies, with at least three animals sampled for each brain region, significant increases in cerebrovascular permeability−surface area products (PAs) determined from 60 s perfusion data for brain uptake in selected regions of the brain where the BBB generally restricts the free passage of blood-borne agents. The data suggested that Taxol was not retained in the rat brain with increasing time; only minimal amounts (2.5% of total control) were detectable in various regions of the brain. Approximately 6−8% of the total control was retained in the brain for Tx-67, suggesting that this chemically modified taxane was able to cross the BBB.

Discussion

We have previously demonstrated that Pgp is expressed in primary cultures of BMECs.[20] Other researchers have demonstrated that Taxol does not cross the endothelial lining of the in vivo BBB due to the presence of Pgp[12−14] localized on the blood-facing surface.[23] A potential approach to overcoming the BBB and achieving delivery of Taxol into the brain is to inhibit Pgp, a strategy that has been well demonstrated by Fellner et al.[13] and Kemper et al.[14] Analogues of CSA as inhibitors of Pgp, for instance, enhance brain Taxol levels by about 3-fold in mice and rats.[13,14] An alterna-

tive approach is to introduce chemical modifications that reduce interactions of Taxol with Pgp to achieve the same goal of enhanced brain levels. Examples in which this latter approach may be productive have been reported for Taxol derivatives in both Pgp-expressing cells in vitro and in drug resistant tumors in mice.[24−27] Thus, our goal was to identify a taxane that could avoid Pgp at the BBB and achieve enhanced brain levels. Tx-67 is a Taxol derivative that has not been examined in any previous study for interactions with Pgp in cell or animal models.

Significant numbers of taxanes were generated by combinatorial chemistry techniques[17] and tested for cytotoxicity and interactions with Pgp by a rhodamine 123 assay. We were able to identify select taxanes such as Tx-67 which retained cytotoxic effects against the breast cancer cell line MCF7 with an IC_{50} of 37.3 nM, an efficacy that was comparable to Taxol, with an IC_{50} of 1.8 nM in the MCF7 cell line.[17] In this study, Tx-67 exhibited no effect on rhodamine 123 uptake, suggesting no interactions with Pgp. Since the rhodamine 123 assay was an indirect indicator of Tx-67 interactions with Pgp, further studies were conducted to look at the transcellular transport of Tx-67 relative to Taxol both in vitro and in situ.

Our data support the previous findings that Pgp is localized to the apical side of the BMECs,[23] as indicated by the asymmetric permeation of Taxol across the monolayers. Taxol permeation across BMEC monolayers was saturable and increased by the typical Pgp inhibitor CsA.[28] Moreover, results indicated that Taxol permeation was increased more effectively when CsA was applied to the apical surface of the monolayers. These observations are entirely consistent with the behavior of Taxol in other recent studies demonstrating the role of Pgp in limiting access of CsA or its analogues into the brain.[12−14]

In contrast to Taxol, the permeation rates for Tx-67 exceeded those of the parent agent at all concentrations examined in vitro. In fact, the asymmetric permeation of Tx-67 across BMEC monolayers favored the apical-to-basolateral passage, even at low concentrations where Taxol was subject to the influence of Pgp. Taxol and the typical Pgp inhibitor, CsA, failed to affect Tx-67 permeation across BMEC monolayers as further evidence that the influence of efflux mechanisms was substantially reduced and or absent completely.

The in situ rat brain perfusion data correlated well with the in vitro permeability data. Our Taxol data was also comparable to other perfusion data typical of other anticancer drugs, such as vincristine and vinblastine, which penetrate the BBB poorly due in part due to the presence of Pgp.[29] However, the PAs and P_{app}s for Tx-67 were substantially improved over Taxol permeation into all rat brain regions sampled. The Tx-67 data were consistent with other reports in which certain newly synthesized taxane analogues have increased absorption and decreased interactions with P-glycoprotein in absorption models and tumor cell lines when modified in C7 and C10 positions on the Taxol structure.[24−27] However, that we are aware, this study is the first to demonstrate a C10-modified taxane with improved distribution across the BBB without the coadministration of Pgp inhibitors.

In other recent studies, colleagues have provided pharmacological evidence that Tx-67 but not Taxol is able to enter brain tissue. Li et al.[30] have shown that Taxol stabilized cyclin-dependent kinase 5 activator (cdk5) (p35) and decreased β-amyloid peptide toxicity ($A\beta_{25-35}$ and $A\beta_{1-42}$) in cortical neuron cultures generated from untreated mice. However, when mice were acutely pretreated with equivalent amounts (i.e., administered i.p. 8 mg/kg every 2 days for 16 days) of either Taxol or Tx-67, Aβ-induced cdk5 activation in subsequently dissociated cortical neuron cultures was blocked only in the neurons from the Tx-67-pretreated animals and not from the Taxol-pretreated animals. These findings imply that the efficacy of Tx-67 in mice was due to improved BBB penetration and entry into neuronal tissue, which provided the block of attempted cdk5 activation in the dissociated neurons in culture by Aβ peptides.[30]

In summary, our studies have demonstrated that a taxane analogue, Tx-67, can be generated with reduced interactions with Pgp at the BBB. Tx-67 appears to cross the BBB both in vitro and in situ by avoiding Pgp interactions, perhaps by exploiting an alternative influx transport mechanism that facilitates passage movement of the agent across the endothelium. As is supported by reports for absorption and distribution into tumor cells,[24−27] our Tx-67 permeation studies are consistent with a hypothesis that the approach of incorporating chemical modifications into Pgp substrates, e.g., taxanes, can enhance permeation across the BBB.

Acknowledgment. This work was supported by a grant from the National Cancer Institute (1 RO1 CA82801) and the Department of the Army through a Research Predoctoral Fellowship (DAMD17-99-1-92430) to Y.L.

References

(1) Taxus: The genus *Taxus*. In *Medicinal and Aromatic Plants—Industrial Profiles*; Itokawa, H., Lee, K.-H., Eds.; Taylor & Francis: London, 2003.
(2) Kingston, D. G. I.; Jagtap, P. G.; Yuan, H.; Samala, L. The Chemistry of Taxol and Taxol Related Taxoids. In *Progress in the Chemistry of Natural Products*; Herz, W., Falk, H., Kirby, G. W., Eds.; Springer: Wien, 2002; pp 56−225.
(3) *Taxane Anticancer Agents: Basic Science and Current Status*; Georg, G. I., Chen, T. T., Ojima, I., Vyas, D. M., Eds.; ACS Symposium Series 583; American Chemical Society: Washington, DC, 1995.
(4) *Taxol Science and Applications*; Suffness, M., Ed.; CRC: Boca Raton, FL, 1995.
(5) The Chemistry and Pharmacology of Taxol and Its Derivatives; Farina, V., Ed.; Elsevier: Amsterdam, 1995.
(6) Jordan, M. A.; Toso, R. J.; Thrower, D.; Wilson, L. Mechanism of mitotic block and inhibition of cell proliferation by Taxol at low concentrations. *Proc. Natl. Acad. Sci. U.S.A.* **1993**, *90*, 9552−9556.
(7) Schiff, P. B.; Fant, J.; Horwitz, S. B. Promotion of microtubule assembly *in vitro* by Taxol. *Nature* **1979**, *277*, 665−667.
(8) Parness, J.; Horwitz, S. B. Taxol binds to polymerized tubulin in vitro. *J. Cell Biol.* **1981**, *91*, 479−487.
(9) Blagosklonny, M. V.; Fojo, T. Molecular effects of paclitaxel: Myths and reality (a critical review). *Int. J. Cancer* **1999**, *83*, 151−156.
(10) Eiseman, J. L.; Eddington, N. D.; Leslie, J.; MacAuley, C.; Sentz, D. L.; Zuhowski, M.; Kujawa, J. M.; Young, D.; Egorin, M. J. Plasma pharmacokinetics and tissue distribution of paclitaxel in CD2F1 mice. *Cancer Chemother. Pharmacol.* **1994**, *34*, 465−471.
(11) Anderson, C. D.; Wang, J.; Kumar, G. N.; McMillan, J. M.; Walle, U. K.; Walle, T. Dexamethasone induction of Taxol metabolism in the rat. *Drug. Metab. Dispos.* **1995**, *23*, 1286−1290.
(12) van Asperen, J., Mayer, U., van Tellingen, O., Beijnen, J. H. The functional role of P-glycoprotein in the blood−brain barrier. *J. Pharm. Sci.* **1997**, *86*, 881−884.

(13) Fellner, S.; Bauer, B.; Miller, D. S.; Schaffrik, M.; Frankhanel, M.; Sprub, T.; Berhardt, G.; Graeff, C.; Farber, L.; Gschaidmeier, H.; Buschauer, A.; Fricker, G. Transport of paclitaxel (Taxol) across the blood−brain barrier in vitro and in vivo. *J. Clin. Invest.* **2002**, *110*, 1309−1318.
(14) Kemper, E. M.; van Zandbergen, A. E.; Cleypool, C.; Mos, H. A.; Boogerd, W.; Beijnen, J. H.; van Tellingen, O. Increased penetration of paclitaxel into the brain by inhibition of P-glycoprotein. *Clin. Cancer Res.* **2003**, *9*, 2849−2855.
(15) Ojima, I.; Duclos, O.; Dorman, G.; Simonot, B.; Prestwich, G. D.; Rao, S.; Lerro, K. A.; Horwitz, S. B. A new paclitaxel photoaffinity analogue with a 3-(4-benzoylphenyl)propanoyl probe for characterization of drug-binding sites on tubulin and P-glycoprotein. *J. Med. Chem.* **1995**, *38*, 3891−3894.
(16) Datta, A.; Hepperle, M.; Georg, G. I. Selective deesterification studies on taxanes: Simple and efficient hydrazinolysis of C-10 and C-13 Ester Functionalities. *J. Org. Chem.* **1995**, *60*, 761−763.
(17) Liu, Y.; Boge, T. C.; Victory, S.; Ali, S. M.; Zygmunt, J.; Georg, G. I.; Marquez, R. T.; Himes, R. H. A systematic SAR study of C10 modified paclitaxel analogues using a combinatorial approach. *Combi. Chem. High Through. Screen* **2002**, *5*, 39−48.
(18) Audus, K. L.; Ng, L.; Wang, W.; Borchardt, R. T. Brain microvessel endothelial cell culture systems. In *Model Systems for Biopharmaceutical Assessment of Drug Absorption and Metabolism*; Borchardt, R. T., Smith, P. L., Wilson, G., Eds.; Plenum: New York, 1996; pp 239−258.
(19) Audus, K. L.; Rose, J. M.; Wang, W.; Borchardt, R. T. Brain microvessel endothelial cell culture systems. In *An Introduction to the Blood−Brain Barrier: Methodology and Biology*; Pardridge, W., Ed.; Cambridge University: Cambridge, 1998; pp 86−93.
(20) Rose, J. M.; Peckham, S. L.; Scism, J. L.; Audus, K. L. Evaluation of the role of P-glycoprotein in ivermectin uptake by primary cultures of bovine brain microvessel endothelial cells. *Neurochem. Res.* **1998**, *23*, 203−209, 1998.
(21) Adson, A.; Raub, T. J.; Burton, P. S.; Barsuhn, C. L.; Hilgers, A. R.; Audus, K. L.; Ho, N. F. H. Quantitative approaches to delineate paracellular diffusion in cultured epithelial cell monolayers. *J. Pharm. Sci.* **1994**, *83*, 1529−1536.
(22) Smith, Q. R.; Allan, D. D. In situ brain perfusion technique. In *The Blood−Brain Barrier*; Nag, S., Ed.; Humana Press: Totowa, NJ, 2003; pp 209−218.
(23) Bendayan, R.; Lee, G.; Bendayan, M. Functional expression and localization of P-glycoprotein at the blood−brain barrier. *Microsc. Res. Technol.* **2002**, *57*, 365−380.
(24) Ojima, I.; Slater, J. C.; Michaud, E.; Kuduk, S. D.; Bounaud, P. Y.; Vrignaud, P.; Bissery, M. C.; Veith, J. M.; Pera, P.; Bernacki, R. J. Syntheses and structure−activity relationships of the second-generation antitumor taxoids: Exceptional activity against drug-resistant cancer cells. *J. Med. Chem.* **1996**, *39*, 3889−3896.
(25) Ojima, I.; Bounaud, P. Y.; Ahern, D. G. New photoaffinity analogues of paclitaxel. *Bioorg. Med. Chem. Lett.* **1999**, *9*, 1189−1194.
(26) Vredenburg, M. R.; Ojima, I.; Veith, J.; Pera, P.; Kee, K.; Cabral, F.; Sharma, A.; Kanter, P.; Greco, W. R.; Bernacki, R. J. Effects of orally active taxanes on P-glycoprotein modulation and colon and breast carcinoma drug resistance. *J. Natl. Cancer Inst.* **2001**, *93*, 1234−1245.
(27) Shionoya, M.; Jimbo, T.; Kitagawa, M.; Soga, T.; Tohgo, A. DJ-927, a novel oral taxane, overcomes P-glycoprotein-mediated multidrug resistance in vitro and in vivo. *Cancer Sci.* **2003**, *94*, 459−466.
(28) Cordon-Cardo, C.; O'Brien, J. P.; Casals, D.; Rittman-Grauer, L.; Biedler, J. L.; Melamed, M. R.; Bertino, J. R. Multidrug-resistance gene (P-glycoprotein) is expressed by endothelial cells at blood−brain barrier sites. *Proc. Natl. Acad. Sci. U.S.A.* **1989**, *86*, 695−698.
(29) Greig, N. H.; Soncrant, T. T.; Shetty, H. U.; Momma, S.; Smith, Q. R.; Rapoport, S. I. Brain uptake and anticancer activities of vincristine and vinblastine are restricted by their low cerebrovascular permeability and binding to plasma constituents in rat. *Cancer Chemother. Pharmacol.* **1990**, *26*, 263−268.
(30) Li, G.; Faibushevich A.; Turunen, B. J.; Yoon, S. O.; Georg, G.; Michaelis, M. L.; Dobrowsky, R. T. Stabilization of the cyclin-dependent kinase 5 activator, p35, by paclitaxel decreases β-amyloid toxicity in cortical neurons. *J. Neurochem.* **2003**, *84*, 347−362.

JM040114B